Published online 1 April 2007

Nucleic Acids Research, 2007, Vol. 35, No. 8 ***2513–2521***
doi:10.1093/nar/gkm125

NXF2 is involved in cytoplasmic mRNA dynamics through interactions with motor proteins

Keizo Takano[1], Takashi Miki[2], Jun Katahira[1,2,*] and Yoshihiro Yoneda[1,2]

[1]Department of Cell Biology and Neuroscience, Graduate School of Medicine, Osaka University, 2-2 Yamadaoka, Suita, Osaka 565-0871, Japan and [2]Laboratories for Biomolecular Networks, Department of Frontier Biosciences, Graduate School of Frontier Biosciences, Osaka University, 1-3 Yamadaoka, Suita, Osaka 565-0871, Japan

Received October 20, 2006; Revised February 13, 2007; Accepted February 14, 2007

ABSTRACT

Tap/NXF1, the founding member of the evolutionarily conserved NXF (Nuclear RNA export Factor) family of proteins, is required for the nuclear export of bulk poly(A)$^+$ RNAs. In mice, three additional NXF family genes (NXF2, NXF3, NXF7) have been identified and characterized to date. Cumulative data suggest that NXF family members play roles, not only in nuclear mRNA export, but also in various aspects of post-transcriptional mRNA metabolism. In order to better understand the functional role of NXF2, we searched for its binding partners by yeast two-hybrid screening and identified several cytoplasmic motor proteins, including KIF17. The interaction of NXF2 with KIF17, which was confirmed by GST pull-down and co-immunoprecipitation assays, is mediated by the N-terminal domain of NXF2, which is required for the punctate localization patterns in dendrites of primary neurons. We also found that the NXF2-containing dendritic granules, which were co-localized with KIF17, mRNA and Staufen1, a known component of neuronal mRNA granules, moved bidirectionally along dendrites in a microtubule-dependent manner. These results suggest that NXF2, a nucleo-cytoplasmic mRNA transporter, plays additional roles in the cytoplasmic localization of mRNAs through interactions with cytoplasmic motor proteins.

INTRODUCTION

The nuclear envelope segregates eukaryotic cells into two major compartments, the nucleus and the cytoplasm. Macromolecules, including proteins and RNAs, are thus transported through the nuclear pore complexes (NPCs) to the location where they function. The past years have seen great progress in the characterization of the export pathways of different classes of RNAs and the identification of protein factors that are involved. Tap/NXF1, a mammalian homolog of yeast Mex67p, is required for the nuclear export of bulk poly(A)$^+$ RNAs (1–6). In the nucleus, precursor mRNA transcripts undergo various processing steps to become fully matured messenger ribonucleoproteins (mRNPs). A series of proteins such as Aly/REF and serine/arginine-rich (SR) proteins bind mRNAs during the processing steps and play a pivotal role in nuclear export (7–10). Tap/NXF1 recognizes the mRNA-binding proteins and facilitates the translocation of bound mRNPs through NPCs via its ability to interact with FG-repeat-containing nucleoporins (5–7,11,12).

Tap/NXF1 is a member of evolutionarily conserved NXF (Nuclear RNA eXport Factor) family of proteins. NXF family proteins, which are encoded on at least four genes in mice (Tap/NXF1, NXF2, NXF3, NXF7), show significant homology to each other and share a similar domain organization (13–18). We, as well as others, have reported that, as shown for Tap/NXF1, NXF2 unequivocally acts as a *bona fide* mRNA exporter (13,16–19). In addition, it has been suggested that NXF2 may have some additional cytoplasmic roles due to its subcellular localization pattern (17,18). Indeed, based on the recent identification of the interaction of NXF2 with fragile X mental retardation protein (FMRP), it appears that NXF2 may regulate the nulceo-cytoplasmic transport or the subsequent translational steps of specific mRNAs in male germ cells and neurons (20).

In order to investigate the role of NXF2 more precisely, we searched for binding partners of NXF2 by yeast two-hybrid screening. Several motor proteins including KIF9, KIF17 and DyneinLC1-like protein were identified. Of these, we focused on KIF17 and demonstrated that NXF2 actually interacts with KIF17 *in vivo* and *in vitro*. In addition, in transiently transfected rat hippocampal neurons, NXF2 showed a punctate localization pattern in neuronal processes. The NXF2-containing particles are co-localized with KIF17 as well as mRNAs and Staufen1 and the N-terminal domain of NXF2 is responsible for both its co-localization and interaction

*To whom correspondence should be addressed. Tel: +81-6-6879-4606; Fax: +81-6-6879-4609; Email: katahira@anat3.med.osaka-u.ac.jp
Correspondence may also be addressed to Yoshihiro Yoneda. Tel: +81-6-6879-4605; Fax: +81-6-6879-4609; Email: yyoneda@anat3.med.osaka-u.ac.jp

© 2007 The Author(s)
This is an Open Access article distributed under the terms of the Creative Commons Attribution Non-Commercial License (http://creativecommons.org/licenses/by-nc/2.0/uk/) which permits unrestricted non-commercial use, distribution, and reproduction in any medium, provided the original work is properly cited.

with KIF17. These data indicate that NXF2 plays an important role in cytoplasmic mRNA localization, in addition to its established function in mRNA nuclear export.

MATERIALS AND METHODS

Constructions of expression vectors

The cloning of the NXF2 cDNA and the construction of GFP-NXF2 and his-NXF2 have been described previously (17). Expression vectors for his-tagged NXF2 deletion mutants, i.e. NXF2-(N), NXF2-(N + LRR), NXF2-(M + C), NXF2-Δ1 and NXF2-Δ2, were generated by inserting PCR-amplified cDNA fragments encoding amino acids 1–270, 1–440, 441–692, 15–692 and 215–692 of NXF2 into the pRSET vector (Invitrogen). A cDNA encoding full-length NXF2 was subcloned into pGBKT7 (Clontech). The resulting plasmid designated pGBKT7-NXF2 encodes a Gal4 DNA-binding domain (DBD)–NXF2 fusion protein and was used as bait in the yeast two-hybrid screening. FLAG-tagged NXF2 was generated by inserting a PCR-amplified DNA fragment encoding full-length NXF2 into the pCMV-FLAG vector, which had been constructed by replacing the EGFP cDNA in the pEGFPC1 vector (Clontech) with an annealed oligonucleotide pair encoding the FLAG-tag sequence. A mammalian expression vector for monomeric red fluorescent protein (mRFP)-tagged NXF2 was generated by inserting the full-length NXF2 cDNA into the pmRFP-C1 vector. To generate pBluescript-KIF17, a cDNA encoding KIF17 was cloned from a mouse cDNA library by PCR and subcloned into the pBluescript KS vector (Stratagene). To generate HA-KIF17, KIF17 cDNA in pBluescript-KIF17 was isolated by treatment with restriction enzymes and inserted into the pCMV-C1-HA vector, which had been constructed by replacing the EGFP cDNA in the pEGFPC1 vector with an annealed oligonucleotide pair encoding the HA-tag sequence. The construction of a mammalian expression vector of mRFP-tagged Staufen1 protein (mRFP-Stau1) will be described elsewhere (T.M. *et al.* submitted for publication) The mammalian expression vectors GFP-NXF2(N), GFP-NXF2-Δ1, GFP-NXF2-Δ2, and NXF2-M + C were generated by inserting PCR-amplified cDNA fragments of NXF2 (each encoding amino acids 1–270, 15–692, 215–692 and 441–692 of NXF2) into the pEGFPC1 vector. The partial cDNA encoding the amino acids 799–1038 of KIF17 was isolated from the two-hybrid positive clone and was subcloned into the pGEX6P2 vector (GE Healthcare) to obtain pGEX-KIF17-C.

Yeast two-hybrid screening

The yeast strain AH109 harboring the pGBKT7-NXF2 bait plasmid was transformed with a mouse testis cDNA library (Clontech). In total, 5.7×10^5 transformants were obtained, of which 80 colonies grew on SDC (-leu, -trp, -his, -ade) plates. These colonies were tested for *MEL1* gene activity by an *in vivo* X-α-Gal agar plate assay according to the manufacturer's protocol. Prey plasmids of positive clones were retransformed in yeast together with pGBKT7-NXF2 to confirm the interactions. As a control, the empty pGBKT7 plasmid was used. Plasmid DNAs of positive clones were recovered and their inserts were analyzed by DNA sequencing.

GST pull-down assay

GST-KIF17-C was expressed in *E.coli* strain BL21(DE3) harboring pGEX-KIF17-C and purified, as described previously (6). ^{35}S-labeled NXF2 was obtained using an *in vitro* transcription–translation system (Promega). The *in vitro* translation mixture was diluted with transport buffer (21) containing 0.5% Triton X-100 and mixed with glutathione-sepharose beads (GE healthcare), to which purified GST-KIF17-C had been pre-adsorbed. After incubation at 4°C for 2 h, the beads were washed four times with transport buffer containing 0.5% Triton X-100 and the bound proteins were released by boiling in SDS-PAGE sample buffer. Purified GST adsorbed on glutathione-sepharose beads was used as a negative control. The bound proteins were separated by SDS-PAGE and visualized using a Bio-Imaging analyzer (Fuji Film). The deletion analysis was performed as described above using a series of pRSET vectors encoding various fragments of NXF2.

Co-immunoprecipitation assay

HEK293T cells were cultured in DMEM (Sigma) supplemented with heat-inactivated 10% fetal bovine serum (GIBCO) at 37°C in 5% CO_2. The FLAG-NXF2 and HA-KIF17 plasmids were co-transfected to 293T cells using the effectene transfection reagent (Qiagen) according to the manufacturer's protocol. At 48 h after transfection, the cells were harvested, washed twice with phosphate buffered saline (PBS) and lysed in ice-cold lysis buffer [20 mM Tris-HCl pH 8.0, 150 mM NaCl, 1 mM EDTA and 1% (v/v) Nonidet P-40] supplemented with protease inhibitors (100 μM phenylmethylsulfonyl fluoride, 10 μg/ml leupeptin, 10 μg/ml aprotinin and 10 μg/ml pepstatin A). To exclude the possibility that co-precipitated RNAs mediate the interaction, RNase A was added to a final concentration of 2 μg/ml. The following steps were carried out at 4°C. After incubating the cell lysates for 15 min at 4°C, insoluble material was removed by centrifugation at $20\,000 \times g$ for 30 min. The supernatants were diluted with an equal volume of lysis buffer without Nonidet P-40 and mixed with 50 μl of anti-FLAG agarose beads (Sigma). The mixtures were incubated for 2 h on a turning wheel. The beads were washed four times with washing buffer [20 mM Tris-HCl, pH 8.0, 150 mM NaCl, 1 mM EDTA and 0.1%(v/v) Nonidet P-40] and the bound material was eluted by boiling in SDS-PAGE sample buffer. Protein samples were resolved by SDS-PAGE and transferred to nitrocellulose membranes. The resulting membranes were blocked for 1 h in PBS containing 5% skim milk and incubated with anti-FLAG M2 antibodies (Sigma, used at 1:1000 dilution) at 4°C for overnight. After washing three times in TBST [20 mM Tris-HCl (pH 7.4), 150 mM NaCl, 0.05% Tween 20], the membranes were further incubated with horseradish-peroxidase-conjugated goat anti-rabbit IgG

(Bio-Rad, used at 1:1000 dilution) at room temperature. After washing three times in TBST, the blots were incubated with ECL Reagent (GE healthcare) and the protein bands were visualized by exposing the blots to X-ray films (Fuji Photo Film Co.)

Primary cultures of rat hippocampal neurons and transfection

Primary cultures of neurons were prepared from hippocampi of embryonic day 18 Sprague–Dawley rats using a previously described method (22). The cells were plated on polyethylenimine (Sigma, P2636)-coated coverslips or glass bottom dishes (Matsunami) at a density of 2.5×10^4 cells/cm^2. Cells were cultured in Neurobasal medium (Invitrogen) supplemented with 2.5 mM L-glutamine (Invitrogen), B-27 (Invitrogen, used at 1:50 dilution), and antibiotics/antimycotic (Invitrogen, used at 1:100 dilution). Dissociated cell cultures at 10–14 days *in vitro* were transfected with DNA constructs using TransMessenger^{TM} Transfection Reagent (Qiagen). The reagent was originally designed for RNA transfection, but it was used here for the DNA transfection of primary neurons instead of mRNA in the protocol. The transfected cells were used for immunocytochemistry or imaging experiments at 24 h after transfection.

Immnocytochemistry and cell labeling experiments

For immunostaining of cultured neurons, cells were fixed by 4% paraformaldehyde in PBS for 10 min. After permeabilization with 0.2% TritonX-100 in PBS for 5 min and blocking with 5% BSA in PBS, the cells were incubated overnight at 4°C with anti-HA antibody (Sigma) at a 1:100 dilution. The cells were subsequently incubated with Alexa 488-conjugated anti-rabbit IgG (Molecular Probes) for 1 h at room temperature. RNA labeling with ethidium bromide (EtBr) was performed as described previously (23). RNase treatment was conducted by incubating neurons with 20 μg/ml RNase A for 15 min after EtBr staining. Fluorescent images of cultured neurons were taken using a confocal laser-scanning microscope attached to an inverted microscope (Axiovert 100M; Carl Zeiss) with a ×63 NA 1.4 Plan-Apochromat.

In situ hybridization

Cells were washed in PBS and then fixed with 4% paraformaldehyde in PBS for 15 min at 37°C. After permeabilization with 0.2% TritonX-100 in PBS for 5 min, the cells were equilibrated in 2 × SSC for 10 min and hybridized with the Cy3-conjugated oligo-dT probe in hybridization buffer (2 × SSC, 1 mg/ml tRNA, 10% dextransulfate, 25% formamide) overnight at 37°C. The cells were washed twice with 2 × SSC and once with 0.5 × SSC at 37°C. Cells that had been pre-treated with RNase A were also used for hybridization to confirm specificity.

In situ hybridization for calcium/calmodulin-dependent protein kinase II (CaMKIIα) was essentially carried out as described previously (24) using a digoxygenin (DIG)-labeled anti-sense ribonucleotide probe encoding a part of the 3′UTR (nt 691–1479) of CaMKIIα mRNA (25). Hybridization and GFP-NXF2 were detected using a mouse anti-DIG Fab fragment and rabbit anti-GFP antibody, respectively. A DIG-labeled sense probe was used for hybridization to confirm the specificity.

Time-lapse imaging and data analysis

For time-lapse imaging, primary neurons were cultured on glass bottom dishes (Matsunami) and the culture media were supplemented with 20 mM HEPES (pH 7.3). Experiments were performed at 37°C maintained by an Air Stream incubator (ASI400; Nevtek). Time-lapse imaging was performed using a confocal laser-scanning microscope as above and the images acquired were processed using the LSM510 software.

For quantification of the dynamics of NXF2-containing granules, we measured the maximum speed of 53 different granules as described previously (24). To calculate the average speed, we tracked 20 randomly chosen unidirectionally moving granules with 26 velocities.

RESULTS

NXF2 interacts with motor proteins

In an initial attempt to investigate the function of NXF2, we searched for binding partners of the protein. To accomplish this, we performed a yeast two-hybrid screening on a mouse testis cDNA library using full-length NXF2 as the bait. Of the 5.7×10^5 clones screened, 80 positive clones were obtained. After sequencing analysis, we found that clones containing partial cDNAs of KIF9, KIF17 and DyneinLC1-like protein were included (Figure 1A). The prey plasmids obtained by the initial screening were rescued from the yeast cells and re-introduced into the yeast AH109 strain. The transformants were tested for growth on synthetic medium lacking leucine, tryptophan, adenine and histidine and the expression of *MEL1* gene activity (Figure 1B). The yeast cells co-expressing GAL4 DBD-NXF2 and GAL4 AD-motor fusion proteins grew well and showed strong *MEL1* gene activity, whereas control yeast cells expressing only GAL4 DBD, together with GAL4AD-motor fusion proteins did not. These data indicate that the cytoplasmic motor proteins are candidates for binding partners of NXF2.

The prey plasmids contain partial cDNAs encoding amino acids 427–779 of KIF9, 779–1038 of KIF17 and 1–90 of DyneinLC1-like protein, respectively. KIF9 and KIF17 belong to the N-terminal motor type kinesins, the motor domains of which are located at their N-termini (26–28). A partial cDNA of KIF17 obtained by this screening encodes the extreme C-terminal region, which includes the cargo-binding domain (27). The DyneinLC1-like protein shows a 93% identity at the amino acid level to DyneinLC1, which is a component of the Dynein motor complex (29–31). We searched for the consensus sequence among these different binding candidates, which may be involved in interactions with NXF2, but failed to find significant sequence homology.

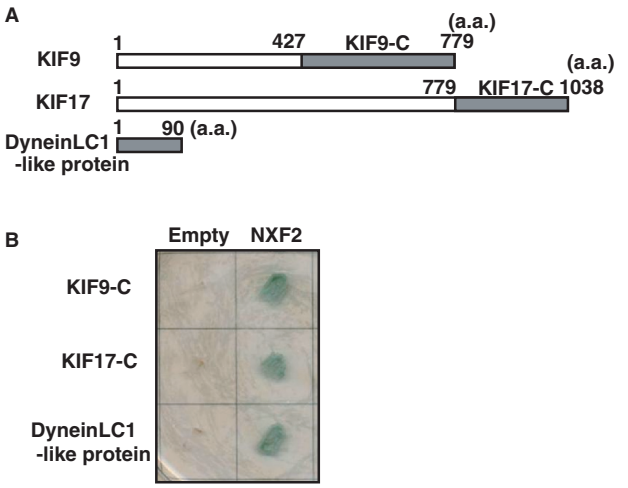

Figure 1. NXF2 interacts with motor proteins. (**A**) A schematic representation of NXF2- binding proteins identified by yeast two-hybrid screening. Each gray-colored box represents partial cDNA inserts obtained by the screening. The protein fragments encoded by the partial cDNAs of KIF9 and KIF17 are designated as KIF9-C and KIF17-C, respectively. Numbers above the boxes indicate amino acid positions. (**B**) Growth and *MEL1* gene expression of transformants co-expressing the NXF2 bait and each prey plasmid identified by the screening. The transformants were grown on selective medium (SD/-Leu/-Trp/-Ade/-His + X-α-Gal). Gal4-DBD alone (Empty) was used as a negative control. The *MEL1* gene expression was examined by *in vivo* X-α-Gal agar plate assay.

Among the binding candidates identified we were not able to obtain a sufficient amount of recombinant KIF9, due to its instability and insolubility in *E. coli* cells. On the other hand, it is so far unclear if DyneinLC1-like protein actually acts as a component of the Dynein motor complex as DyneinLC1, although they show a significant sequence similarity. In contrast, it is well established that KIF17 acts as a cytoplasmic motor and that in brain, both NXF2 and KIF17 are expressed in hippocampal neurons (20,27). Therefore, in the next step, we concentrated on the interaction between NXF2 and KIF17 and investigated the biological significance of their interaction in hippocampal neurons.

NXF2 binds KIF17 *in vitro* and *in vivo*

In order to confirm whether NXF2 directly binds KIF17, GST pull-down assays were performed. Purified GST or GST-fused KIF17-C, which contains the partial cDNA isolated from the positive prey plasmid, was pre-adsorbed on glutathione sepahrose beads and *in vitro* translated [^{35}S]-methionine-labeled full-length NXF2 was added. As shown in Figure 2A, GST-KIF17-C specifically pulled-down NXF2, while GST alone did not.

To examine the interactions under *in vivo* conditions, co-immunoprecipitation assays were performed. Cell lysates prepared from HEK293T cells transiently expressing HA-tagged full-length KIF17 with or without FLAG-tagged NXF2 were subjected to immunoprecipitation using an anti-FLAG antibody. As shown in Figure 2B, HA-KIF17 was co-immunoprecipitated only when FLAG-tagged NXF2 was co-expressed and the addition of RNase A in the binding reaction did not abolish the

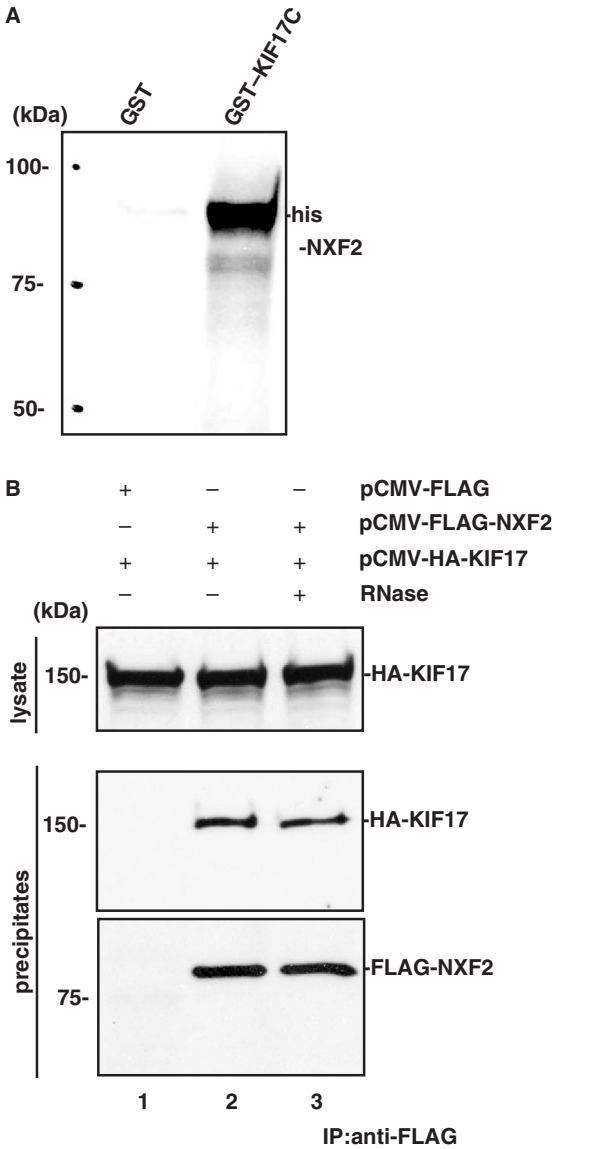

Figure 2. NXF2 binds KIF17 *in vitro* and *in vivo*. (**A**) [^{35}S]-methionine-labeled his-NXF2 protein produced by *in vitro* translation was incubated with bacterially expressed GST or GST−KIF17-C, which had been pre-adsorbed on GSH beads. After washing, the bound proteins were eluted, separated on an SDS-PAGE gel and visualized by fluorography. (**B**) Cell lysates prepared from 293T cells expressing HA-KIF17 with or without FLAG-NXF2 were subjected to immunoprecipitation using anti-FLAG antibody. In lane 3, the cell lysate was pre-treated with RNase A. Immuno-pellets were separated by SDS-PAGE and subjected to immunoblotting using anti-KIF17 or anti-FLAG antibodies.

interaction. (Figure 2B). Thus, we conclude that the interaction of NXF2 with KIF17 is specific and that the interaction occurs between the full-length proteins under *in vivo* condition.

N-domain of NXF2 is required for the interaction with KIF17

To further narrow down the KIF17-binding domain of NXF2, various NXF2 deletion mutants (Figure 3A) were prepared by *in vitro* translation and their interactions with

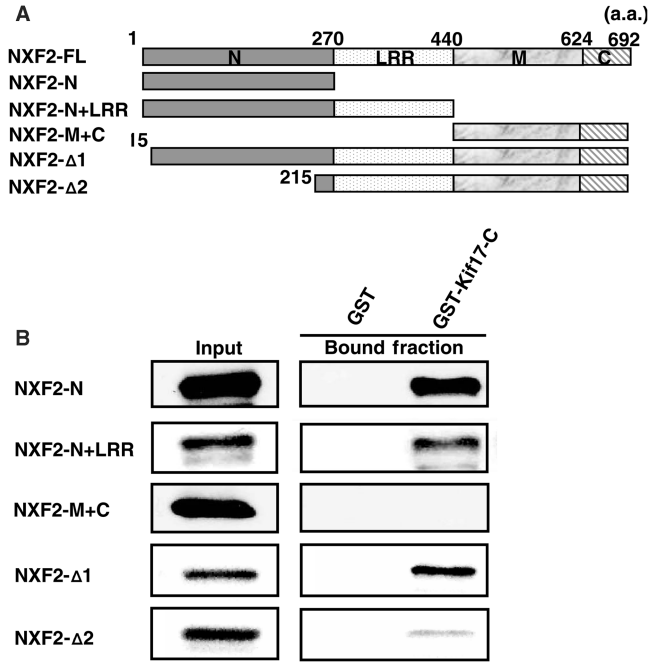

Figure 3. N-domain of NXF2 is required for the interaction with KIF17. (**A**) A schematic representation of the NXF2 deletion mutants used in the experiments. The numbers on top indicate amino acids residue numbers. Fragments containing amino acids 1–269, 1–439 and 440–692 of NXF2 are designated as NXF2-(N), NXF2-(N + LRR) and NXF2-(M + C), respectively. (**B**) NXF2 deletion mutants, produced by *in vitro* translation in the presence of [^{35}S]-methionine, were incubated with bacterially produced GST or GST-KIF17-C, which had been pre-adsorbed on GSH beads. After washing, the bound proteins were eluted, separated on an SDS-PAGE gel and visualized by fluorography. The input lanes contain 18% of the labeled proteins used for the binding reactions.

GST-KIF17-C were examined by GST pull-down assay (Figure 3B). The C-terminal deletion mutants, designated NXF2-N and NXF2-N + LRR, interacted with KIF17, whereas an N-terminal deletion mutant NXF2-M + C did not. Another truncated mutant, NXF2-Δ1, lacking the 15 N-terminal amino acids retained binding activity to KIF17-C, but the binding was dramatically weakened when a further 200 amino acids were deleted from the N-terminal end (NXF2-Δ2). These results indicate that the N-domain of NXF2 is required for interaction with KIF17.

Subcellular localization and dynamic behavior of NXF2 in cultured hippocampal neurons

We examined the subcellular distribution of NXF2 by the transient expression of GFP-NXF2 in cultured rat hippocampal neurons. In primary neurons, GFP-NXF2 was predominantly localized in the nucleus and accumulated at the nuclear rim as described in previous reports (13,14,17,18). Furthermore, GFP-NXF2 was also detected in granular structures in the dendrites of primary neurons (Figure 4A). These granules varied in size and displayed persistent, oscillatory and mobile characteristics. Time-lapse imaging revealed that some of the granules traveled along the dendrites

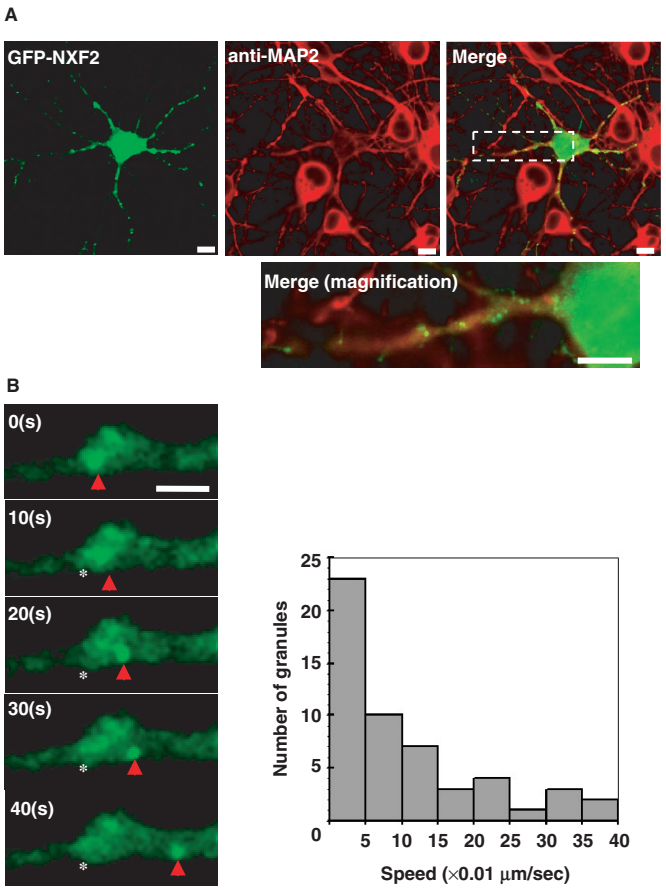

Figure 4. The distribution of NXF2 in primary neurons. (**A**) Rat hippocampal neurons in dissociated cultures were transfected with GFP-NXF2. At 24 h post-transfection, the neurons were immunostained by anti-MAP2 antibody. The images were obtained by fluorescence confocal microscopy. The bottom panel shows a magnified view of the field outlined by the dotted rectangle in the upper right image. Scale bar, 10 μm. (**B**) Left: Time- lapse imaging of GFP-NXF2 in dendrites of primary neurons. The arrowheads indicate a moving granule, whereas the asterisk indicates the position of the granule at the beginning of the observation. Scale bar, 2 μm. Right: Distribution of maximum speed of 60 GFP-NXF2-containing granules.

with an average velocity of 0.13 ± 0.07 μm/s ($n = 26$) and an average maximum speed at 0.10 ± 0.10 μm/s ($n = 53$) (Figure 4B, see also Supplementary Movie 1). When NXF2-expressing cells were treated with nocodazole, a microtubule-depolymerizing agent, the level of mobility of the NXF2-containing granules significantly decreased (see Supplementary Movie 2), suggesting that microtubules are involved in their mobile characteristics.

NXF2 is a component of neuronal RNA granules

It has been reported that, in neurons, different types of mRNAs are transported along dendrites as a component of large macromolecular ribonucleoprotein complexes, which are referred to as RNA granules or transport ribonucleoprotein (RNP) (32,33). The behavior of GFP-NXF2-containing granules in dendrites was very similar to the reported characteristics of RNA granules (34–36). We therefore investigated whether the NXF2-containing

granular structures in dendrites are actually RNA granules. The RNAs were detected by EtBr staining as described previously (23). The NXF2-containing granules showed a high degree of co-localization with the EtBr signals. As expected, the signals for EtBr were completely abolished by RNase A treatment, indicating that RNA is a component of the NXF2-containing granules (Supplementary Data, Figure 1).

To investigate what type of RNAs are components of the NXF2-containing granules, we first performed *in situ* hybridization with oligo(dT) probes. In dendrites, poly(A)$^+$ RNA signals were found in granules, while neurons treated with RNase A before hybridization did not show such signals (data not shown). The signals of poly(A)$^+$ RNAs were partly overlapped with the GFP-NXF2-containing granules (Figure 5A). This indicates that the NXF2 forms complexes with mRNAs. Furthermore, we examined the association of NXF2-containing granules with CaMKIIα mRNA, a known dendritically targeted transcript (24,37,38), by *in situ* hybridization. In contrast, as a negative control, *in situ* hybridization was performed with the sense probe, but no signal was detected in dendrites (data not shown), CaMKIIα mRNA was localized in granules in dendrites as reported previously, however, it was not observed in GFP-NXF2-containing granules (Figure 5B).

We next investigated the issue of whether the NXF2-containing granules are co-localized with Staufen1, a well-known marker protein for neuronal RNA granules. For this, mRFP-tagged Staufen1 (mRFP-Stau1) was co-expressed along with GFP-NXF2. GFP-NXF2 and mRFP-Stau1 were co-localized in granules in dendrites (Figure 5C). These results strongly suggest that NXF2 is a component of the RNA granules in neurons.

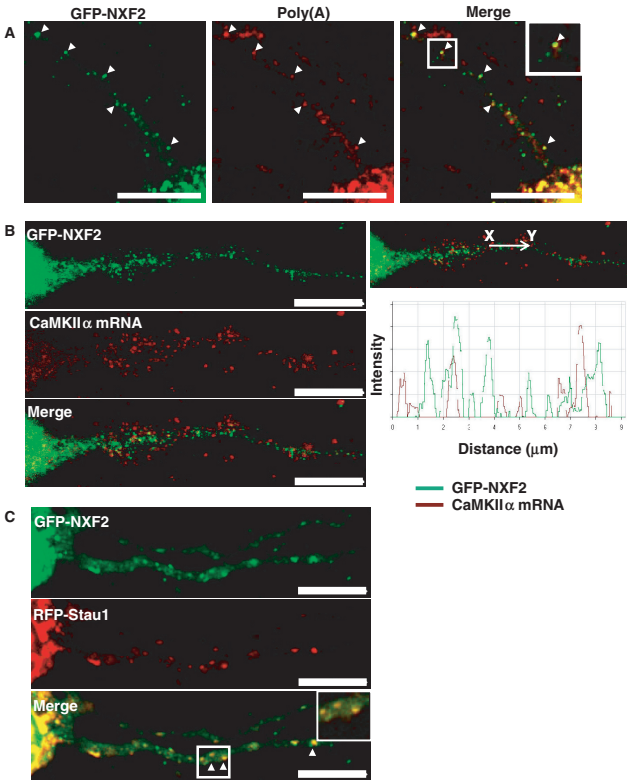

Figure 5. NXF2 co-localizes with the components of RNA granules in dendrites of primary neurons. (**A**) GFP-NXF2-expressing neurons were processed for *in situ* hybridization with Cy3-labeled oligo(dT) probe (red). The insert in the merged image is a blow-up of the region of the image indicated. Scale bars, 10 μm. (**B**) Left: GFP-NXF2-expressing neurons were processed for *in situ* hybridization with a DIG-labeled anti-sense riboprobe for CaMKIIα mRNA. CaMKIIα mRNA was detected by mouse anti-DIG Fab fragment followed by Alexa568-labeled anti-mouse IgG (red), whereas GFP-NXF2 was detected using rabbit anti-GFP followed by Alexa488 labeled anti-rabbit IgG (green). Scale bars, 10 μm. Right: Fluorescent intensity profile along the X–Y axis indicated in the upper right image. (**C**) GFP-NXF2 and mRFP-Stau1 were co-expressed in cultured rat hippocampal neurons and their localizations were observed at 24 h after transfection by fluorescence confocal microscopy. The insert in the merged image is a blow-up of the region of the image indicated. Scale bar, 10 μm.

N-domain of NXF2 is required for the recruitment into RNA granules

We then determined which region of NXF2 is required for its localization in neuronal RNA granules. For this, various NXF2 fragments fused with GFP were expressed in cultured neurons and their subcellular localization was examined. Both GFP-NXF2-N and GFP-NXF2-Δ1 showed granular distributions similar to the full-length protein (Figure 6). In contrast, GFP-NXF2-Δ2 and NXF2-M + C, both of which did not interact with KIF17, was diffusely localized in the cytoplasm, and never showed the punctate localization pattern in dendrites (Figure 6). These data indicate that the N-domain of NXF2 involved in KIF17 interactions, is required for incorporation into RNA granules.

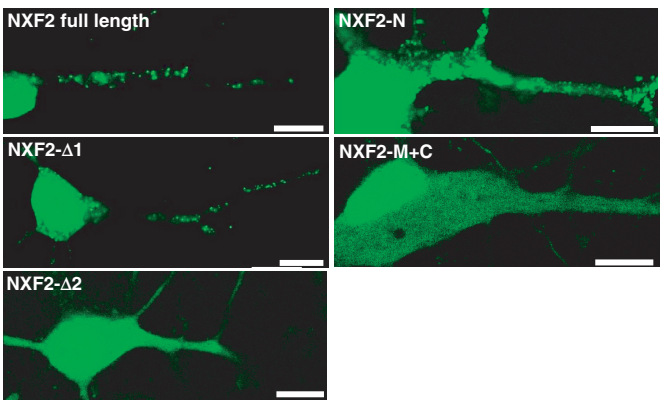

Figure 6. N-domain of NXF2 is required for the recruitment into RNA granules. NXF2 deletion mutants fused to GFP were expressed in rat hippocampal neurons, and their localization in dendrites was observed 24 h after transfection by fluorescence confocal microscopy. Scale bar, 10 μm.

NXF2-containing granules are co-localized with KIF17 in dendrites

It has been reported that KIF17 shows punctate localization patterns in dendrites of hippocampal neurons (27,39–41). We thus investigated whether NXF2-containing granules are co-localized with KIF17 in dendrites. To accomplish this, GFP-NXF2 was co-expressed with HA-KIF17 in primary neurons and

the cells were immunostained with an anti-HA antibody. The GFP-NXF2-containing granules showed a high degree of co-localization with HA-KIF17, indicating that KIF17 is also a component of dendritic NXF2-containing RNA granules (Figure 7).

DISCUSSION

In eukaryotic cells, the organization of the cytoplasm is maintained through the continuous trafficking of different organelles and macromolecular complexes along microtubules and actin microfilaments. Cytoplasmic mRNA localization has been extensively studied because of its importance in the maintenance of cell polarity, specifying germ cells and neuronal plasticity. Numerous motor proteins such as kinesin, dynein and myosin family members are known to be involved in these processes (30,42). KIF17, a recently characterized member of the kinesin protein superfamily, has been shown to transport cargoes, including the N-methyl-D-aspartate (NMDA) receptor and potassium channel Kv4.2 containing vesicles, in neurons (27,41). Here we identified KIF17 as a binding partner of NXF2 by yeast two-hybrid screening. We found that the N-domain of NXF2 interacts with the C-terminal region of KIF17. In some cases, it has been reported that kinesins interact with cargo proteins via PDZ-containing adaptor proteins (27,43). However, the data herein indicate a direct interaction between NXF2 and KIF17, although the possibility that NXF2 might interact with KIF17 through adaptor proteins in the cell lysates cannot be completely excluded. In any case, the interaction between NXF2 and KIF17 demonstrated here is the first report that indicates the molecular link between the NXF RNA export factors and the cytoplasmic motor proteins.

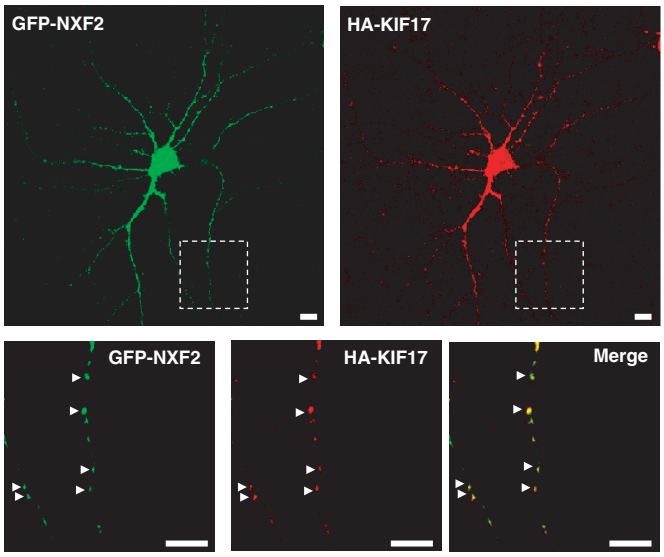

Figure 7. NXF2 co-localizes with KIF17 in dendrites of primary neurons. Rat primary neurons were transfected with GFP-NXF2 and HA-KIF17. At 24 h post-transfection, the neurons were immunostained with anti-HA antibody. The images were obtained by fluorescence confocal microscopy. The upper panels show images of a rat primary neuron expressing GFP-NXF2 and HA-KIF17. The lower panels show magnified views of the field outlined by the dotted rectangle in the upper images. The arrowheads indicate co-localized puncta. Scale bars, 10 μm.

In cultured hippocampal neurons, NXF2 was co-localized with RNAs and Staufen1, a RNA granule marker. The N-domain of NXF2, including the KIF17-binding domain, was required for the localization in the neuronal RNA granules. *In situ* localization revealed that poly(A)$^+$ RNAs were constituents of NXF2-containing granules, but CaMKIIα mRNA was mostly excluded. These observations are consistent with a previous report that CaMKIIα mRNA is transported by KIF5a within dendrites (24). Thus, our observation raises the possibility that NXF2 is involved in the dendritic targeting of yet unknown mRNAs. We further demonstrated that the NXF2-containing granules move along neuronal dendrites bidirectionally in a microtubule-dependent manner. These results suggest that NXF2 may participate in the cytoplasmic dynamics of mRNAs as a component of RNA granules. The average velocity of NXF2-containing granules in neuronal dendrites was found to be ~0.13 μm/s, comparable to values reported for Staufen (~0.1 μm/s) (34), and slightly faster than that of an mRNA reporter with the 3′-UTR of CaMKIIα (0.03 ~ 0.05 μm/s) (36) containing granules. Although most of the NXF2-containing granules were mobile, the average velocity was much slower than that of the KIF17-containing vesicles (~0.76 μm/s) (39).

In this study, we identified KIF9 and the DyneinLC1-like protein as NXF2-binding partners, in addition to KIF17. The binding of NXF2 to the DyneinLC1-like protein was also confirmed using GST pull-down assays (data not shown). Our observation that NXF2- positive granules move bidirectionally could be explained, in part, by the mixed polarity of the dendritic microtubules (44) or alternatively, by the dual interactions of NXF2 with the plus- and minus-end-directed motor proteins. KIF17b has been reported to be heavily phosphorylated in cultured cells and phosphorylation sites are present in the C-terminal region (45) to which NXF2 binds. Therefore, the interaction of NXF2 with different motor proteins might be coordinated by phosphorylation.

It is becoming apparent that mRNA metabolism which takes place in the cytoplasm, i.e. translational control, cytoplasmic localization and decay processes, initially starts in the nucleus. For example, it is known that Y14 and Magoh, predominantly nuclear- RNA-binding proteins and the known components of exon–exon junction complexes (EJCs), affect the fates of bound mRNAs in the cytoplasm (46–48). We, as well as others, have recently demonstrated that NXF2 functions as a *bona fide* exporter of mRNA. Is NXF2 one such 'bi-functional' factor? It has been reported that, *in vitro*, NXF2 shows binding activity to several EJC components, i.e. Magoh and Aly/REF (18), and very recently that NXF2 binds to FMRP, which is implicated in the control of translation as well as the cytoplasmic localization of specific mRNAs (20,49–51). FMRP shows punctate localization patterns in mammalian neuronal cells (52) and the *Drosophila* FMRP-containing granules are moved along cytoplasmic processes of cultured cells bidirectionally by Kinesin-1 and

cytoplasmic dynein (53). We found that the KIF17-binding site required for targeting NXF2 into dendritic RNA granules coincides with the region where FMRP binds. Thus, these findings raise one intriguing possibility. That is, after exporting bound mRNA cargoes into the cytoplasm via interaction with EJC components, NXF2 interacts with FMRP, which maintains the bound mRNAs in a translationally dormant state. The interaction of NXF2 with EJC components and FMRP may be consecutive and required for the formation of NXF2-containing RNA granules. NXF2, along with bound mRNPs, is then recognized by KIF17 and travels along microtubules within dendrites. Thus, it is likely that NXF2, via its affinity for different factors, acts as a bi-functional scaffold to provide a link between the nucleo-cytoplasmic and the intra-cytoplasmic transport of mRNAs. RNA granules are thought to be heterogeneous in nature (37). Indeed, in a mammalian system, FMRP has been identified as a component of RNA granules bound to KIF5b (24). The NXF2-containing RNA granules recognized by KIF17 may represent one such variation. The identification of target mRNAs for NXF2 will help to further substantiate this possibility.

KIF17b, a testis-specific isoform of neuronal KIF17, has been reported to be involved in the regulation of cAMP-response element modulator (CREM)-dependent transcription, the formation of chromatoid bodies via interplay with Argonaute proteins, and the transport of TB-RBP-containing ribonucleoprotein complexes in the cytoplasm of post-meiotic germ cells (40,54–56). The latter two reports suggest that KIF17b is involved in the translational control and/or cytoplasmic transport of haploid specific mRNAs in chromatoid bodies of male germ cells, which are thought to be functionally homologous to the processing bodies (P-bodies) of somatic cells. Given the recent findings that suggest a functional relationship between neuronal RNA granules and P-bodies (37,57), our findings may provide an attractive scenario, in which similar mechanisms operate in the formation and/or the transport of cytoplasmic mRNA-containing granules in neurons.

SUPPLEMENTARY DATA

Supplementary Data are available at NAR Online.

ACKNOWLEDGEMENTS

We wish to thank Drs R. Tsien and T. Nagai for providing the mRFP vector, Dr N. Hirokawa for the generous gift of the cDNA clone for KIF17, Dr Y. Kanai for valuable advice on *in situ* hybridization, and Dr Y. Mori for the generous gift of the cDNA clone for CaMKIIα and helpful advice. We also thank members of Prof. Y. Yoneda's lab, especially Dr M. Sasaki for his help during the initial phase of this project and Mr S. Oe for technical advice on primary cultures of rat hippocampal neurons. This work was supported, in part, by grants from the Japanese Ministry of Education, Culture, Sports, Science, and Technology and the Human Frontier Science Program. Funding to pay the Open Access publication charges for this article was provided by the Japanese Ministry of Education, Culture, Sports, Science and Technology (MEXT).

Conflict of interest statement. None declared.

REFERENCES

1. Katahira,J., Strasser,K., Podtelejnikov,A., Mann,M., Jung,J.U. and Hurt,E. (1999) The Mex67p-mediated nuclear mRNA export pathway is conserved from yeast to human. *EMBO J.*, **18**, 2593–2609.
2. Bear,J., Tan,W., Zolotukhin,A.S., Tabernero,C., Hudson,E.A. and Felber,B.K. (1999) Identification of novel import and export signals of human TAP, the protein that binds to the constitutive transport element of the type D retrovirus mRNAs. *Mol. Cell. Biol.*, **19**, 6306–6317.
3. Kang,Y. and Cullen,B.R. (1999) The human Tap protein is a nuclear mRNA export factor that contains novel RNA-binding and nucleocytoplasmic transport sequences. *Genes Dev.*, **13**, 1126–1139.
4. Bachi,A., Braun,I.C., Rodrigues,J.P., Pante,N., Ribbeck,K., von Kobbe,C., Kutay,U., Wilm,M., Gorlich,D. *et al.* (2000) The C-terminal domain of TAP interacts with the nuclear pore complex and promotes export of specific CTE-bearing RNA substrates. *RNA*, **6**, 136–158.
5. Schmitt,I. and Gerace,L. (2001) In vitro analysis of nuclear transport mediated by the C-terminal shuttle domain of Tap. *J. Biol. Chem.*, **276**, 42355–42363.
6. Katahira,J., Straesser,K., Saiwaki,T., Yoneda,Y. and Hurt,E. (2002) Complex formation between Tap and p15 affects binding to FG-repeat nucleoporins and nucleocytoplasmic shuttling. *J. Biol. Chem.*, **277**, 9242–9246.
7. Le Hir,H., Nott,A. and Moore,M.J. (2003) How introns influence and enhance eukaryotic gene expression. *Trends Biochem. Sci.*, **28**, 215–220.
8. Masuyama,K., Taniguchi,I., Kataoka,N. and Ohno,M. (2004) RNA length defines RNA export pathway. *Genes Dev.*, **18**, 2074–2085.
9. Masuyama,K., Taniguchi,I., Kataoka,N. and Ohno,M. (2004) SR proteins preferentially associate with mRNAs in the nucleus and facilitate their export to the cytoplasm. *Genes Cells*, **9**, 959–965.
10. Huang,Y., Yario,T.A. and Steitz,J.A. (2004) A molecular link between SR protein dephosphorylation and mRNA export. *Proc. Natl. Acad. Sci. USA*, **101**, 9666–9670.
11. Dreyfuss,G., Kim,V.N. and Kataoka,N. (2002) Messenger-RNA-binding proteins and the messages they carry. *Nat. Rev. Mol. Cell. Biol.*, **3**, 195–205.
12. Grant,R.P., Hurt,E., Neuhaus,D. and Stewart,M. (2002) Structure of the C-terminal FG-nucleoporin binding domain of Tap/NXF1. *Nat. Struct. Biol.*, **9**, 247–251.
13. Herold,A., Suyama,M., Rodrigues,J.P., Braun,I.C., Kutay,U., Carmo-Fonseca,M., Bork,P. and Izaurralde,E. (2000) TAP (NXF1) belongs to a multigene family of putative RNA export factors with a conserved modular architecture. *Mol. Cell. Biol.*, **20**, 8996–9008.
14. Herold,A., Klymenko,T. and Izaurralde,E. (2001) NXF1/p15 heterodimers are essential for mRNA nuclear export in Drosophila. *RNA*, **7**, 1768–1780.
15. Jun,L., Frints,S., Duhamel,H., Herold,A., Abad-Rodrigues,J., Dotti,C., Izaurralde,E., Marynen,P. and Froyen,G. (2001) NXF5, a novel member of the nuclear RNA export factor family, is lost in a male patient with a syndromic form of mental retardation. *Curr. Biol.*, **11**, 1381–1391.
16. Yang,J., Bogerd,H.P., Wang,P.J., Page,D.C. and Cullen,B.R. (2001) Two closely related human nuclear export factors utilize entirely distinct export pathways. *Mol. Cell*, **8**, 397–406.
17. Sasaki,M., Takeda,E., Takano,K., Yomogida,K., Katahira,J. and Yoneda,Y. (2005) Molecular cloning and functional characterization of mouse Nxf family gene products. *Genomics*, **85**, 641–653.
18. Tan,W., Zolotukhin,A.S., Tretyakova,I., Bear,J., Lindtner,S., Smulevitch,S.V. and Felber,B.K. (2005) Identification and characterization of the mouse nuclear export factor (Nxf) family members. *Nucleic Acids Res.*, **33**, 3855–3865.

19. Tretyakova,I., Zolotukhin,A.S., Tan,W., Bear,J., Propst,F., Ruthel,G. and Felber,B.K. (2005) Nuclear export factor family protein participates in cytoplasmic mRNA trafficking. *J. Biol. Chem.*, **280**, 31981–31990.
20. Lai,D., Sakkas,D. and Huang,Y. (2006) The fragile X mental retardation protein interacts with a distinct mRNA nuclear export factor NXF2. *RNA*, **12**, 1446–1449.
21. Kotera,I., Sekimoto,T., Miyamoto,Y., Saiwaki,T., Nagoshi,E., Sakagami,H., Kondo,H. and Yoneda,Y. (2005) Importin alpha transports CaMKIV to the nucleus without utilizing importin beta. *EMBO J.*, **24**, 942–951.
22. Brewer,G.J., Torricelli,J.R., Evege,E.K. and Price,P.J. (1993) Optimized survival of hippocampal neurons in B27-supplemented Neurobasal, a new serum-free medium combination. *J. Neurosci. Res.*, **35**, 567–576.
23. Tang,S.J., Meulemans,D., Vazquez,L., Colaco,N. and Schuman,E. (2001) A role for a rat homolog of staufen in the transport of RNA to neuronal dendrites. *Neuron*, **32**, 463–475.
24. Kanai,Y., Dohmae,N. and Hirokawa,N. (2004) Kinesin transports RNA: isolation and characterization of an RNA-transporting granule. *Neuron*, **43**, 513–525.
25. Mori,Y., Imaizumi,K., Katayama,T., Yoneda,T. and Tohyama,M. (2000) Two cis-acting elements in the 3′ untranslated region of alpha-CaMKII regulate its dendritic targeting. *Nat. Neurosci.*, **3**, 1079–1084.
26. Piddini,E., Schmid,J.A., de Martin,R. and Dotti,C.G. (2001) The Ras-like GTPase Gem is involved in cell shape remodelling and interacts with the novel kinesin-like protein KIF9. *EMBO J.*, **20**, 4076–4087.
27. Setou,M., Nakagawa,T., Seog,D.H. and Hirokawa,N. (2000) Kinesin superfamily motor protein KIF17 and mLin-10 in NMDA receptor-containing vesicle transport. *Science*, **288**, 1796–1802.
28. Miki,H., Setou,M., Kaneshiro,K. and Hirokawa,N. (2001) All kinesin superfamily protein, KIF, genes in mouse and human. *Proc. Natl. Acad. Sci. USA*, **98**, 7004–7011.
29. Fuhrmann,J.C., Kins,S., Rostaing,P., El Far,O., Kirsch,J., Sheng,M., Triller,A., Betz,H. and Kneussel,M. (2002) Gephyrin interacts with Dynein light chains 1 and 2, components of motor protein complexes. *J. Neurosci.*, **22**, 5393–5402.
30. Tekotte,H. and Davis,I. (2002) Intracellular mRNA localization: motors move messages. *Trends Genet.*, **18**, 636–642.
31. Mallik,R. and Gross,S.P. (2004) Molecular motors: strategies to get along. *Curr. Biol.*, **14**, R971–R982.
32. Kiebler,M.A. and DesGroseillers,L. (2000) Molecular insights into mRNA transport and local translation in the mammalian nervous system. *Neuron*, **25**, 19–28.
33. Steward,O. and Schuman,E.M. (2003) Compartmentalized synthesis and degradation of proteins in neurons. *Neuron*, **40**, 347–359.
34. Knowles,R.B., Sabry,J.H., Martone,M.E., Deerinck,T.J., Ellisman,M.H., Bassell,G.J. and Kosik,K.S. (1996) Translocation of RNA granules in living neurons. *J. Neurosci.*, **16**, 7812–7820.
35. Kohrmann,M., Luo,M., Kaether,C., DesGroseillers,L., Dotti,C.G. and Kiebler,M.A. (1999) Microtubule-dependent recruitment of Staufen-green fluorescent protein into large RNA-containing granules and subsequent dendritic transport in living hippocampal neurons. *Mol. Biol. Cell*, **10**, 2945–2953.
36. Rook,M.S., Lu,M. and Kosik,K.S. (2000) CaMKIIalpha 3′ untranslated region-directed mRNA translocation in living neurons: visualization by GFP linkage. *J. Neurosci.*, **20**, 6385–6393.
37. Kiebler,M.A. and Bassell,G.J. (2006) Neuronal RNA granules: movers and makers. *Neuron*, **51**, 685–690.
38. Vessey,J.P., Vaccani,A., Xie,Y., Dahm,R., Karra,D., Kiebler,M.A. and Macchi,P. (2006) Dendritic localization of the translational repressor Pumilio 2 and its contribution to dendritic stress granules. *J. Neurosci.*, **26**, 6496–6508.
39. Guillaud,L., Setou,M. and Hirokawa,N. (2003) KIF17 dynamics and regulation of NR2B trafficking in hippocampal neurons. *J. Neurosci.*, **23**, 131–140.
40. Chennathukuzhi,V., Morales,C.R., El Alfy,M. and Hecht,N.B. (2003) The kinesin KIF17b and RNA-binding protein TB-RBP transport specific cAMP-responsive element modulator-regulated mRNAs in male germ cells. *Proc. Natl. Acad. Sci. USA*, **100**, 15566–15571.
41. Chu,P.J., Rivera,J.F. and Arnold,D.B. (2006) A role for Kif17 in transport of Kv4.2. *J. Biol. Chem.*, **281**, 365–373.
42. Martin,K.C. and Zukin,R.S. (2006) RNA trafficking and local protein synthesis in dendrites: an overview. *J. Neurosci.*, **26**, 7131–7134.
43. Setou,M., Seog,D.H., Tanaka,Y., Kanai,Y., Takei,Y., Kawagishi,M. and Hirokawa,N. (2002) Glutamate-receptor-interacting protein GRIP1 directly steers kinesin to dendrites. *Nature*, **417**, 83–87.
44. Baas,P.W., Deitch,J.S., Black,M.M. and Banker,G.A. (1988) Polarity orientation of microtubules in hippocampal neurons: uniformity in the axon and nonuniformity in the dendrite. *Proc. Natl. Acad. Sci. USA*, **85**, 8335–8339.
45. Kotaja,N., Macho,B. and Sassone-Corsi,P. (2005) Microtubule-independent and protein kinase A-mediated function of kinesin KIF17b controls the intracellular transport of activator of CREM in testis (ACT). *J. Biol. Chem.*, **280**, 31739–31745.
46. Farina,K.L. and Singer,R.H. (2002) The nuclear connection in RNA transport and localization. *Trends Cell Biol.*, **12**, 466–472.
47. Hachet,O. and Ephrussi,A. (2004) Splicing of oskar RNA in the nucleus is coupled to its cytoplasmic localization. *Nature*, **428**, 959–963.
48. Palacios,I.M., Gatfield,D., St Johnston,D. and Izaurralde,E. (2004) An eIF4AIII-containing complex required for mRNA localization and nonsense-mediated mRNA decay. *Nature*, **427**, 753–757.
49. Willemsen,R., Oostra,B.A., Bassell,G.J. and Dictenberg,J. (2004) The fragile X syndrome: from molecular genetics to neurobiology. *Ment. Retard. Dev. Disabil. Res. Rev.*, **10**, 60–67.
50. Darnell,J.C., Mostovetsky,O. and Darnell,R.B. (2005) FMRP RNA targets: identification and validation. *Genes Brain Behav.*, **4**, 341–349.
51. Bardoni,B., Davidovic,L., Bensaid,M. and Khandjian,E.W. (2006) The fragile X syndrome: exploring its molecular basis and seeking a treatment. *Expert Rev. Mol. Med.*, **8**, 1–16.
52. Diego Otero,Y., Severijnen,L.A., van Cappellen,G., Schrier,M., Oostra,B. and Willemsen,R. (2002) Transport of fragile X mental retardation protein via granules in neurites of PC12 cells. *Mol. Cell. Biol.*, **22**, 8332–8341.
53. Ling,S.C., Fahrner,P.S., Greenough,W.T. and Gelfand,V.I. (2004) Transport of Drosophila fragile X mental retardation protein-containing ribonucleoprotein granules by kinesin-1 and cytoplasmic dynein. *Proc. Natl. Acad. Sci. USA*, **101**, 17428–17433.
54. Macho,B., Brancorsini,S., Fimia,G.M., Setou,M., Hirokawa,N. and Sassone-Corsi,P. (2002) CREM-dependent transcription in male germ cells controlled by a kinesin. *Science*, **298**, 2388–2390.
55. Kotaja,N., Lin,H., Parvinen,M. and Sassone-Corsi,P. (2006) Interplay of PIWI/Argonaute protein MIWI and kinesin KIF17b in chromatoid bodies of male germ cells. *J. Cell Sci.*, **119**, 2819–2825.
56. Kotaja,N., Bhattacharyya,S.N., Jaskiewicz,L., Kimmins,S., Parvinen,M., Filipowicz,W. and Sassone-Corsi,P. (2006) The chromatoid body of male germ cells: similarity with processing bodies and presence of Dicer and microRNA pathway components. *Proc. Natl. Acad. Sci. USA*, **103**, 2647–2652.
57. Anderson,P. and Kedersha,N. (2006) RNA granules. *J. Cell Biol.*, **172**, 803–808.